

# The postbiotic ReFerm<sup>®</sup> versus standard nutritional support in advanced alcohol-related liver disease (GALA-POSTBIO): a randomized controlled phase 2 trial

Received: 4 May 2024

Accepted: 2 June 2025

Published online: 01 July 2025

 Check for updates

A list of authors and their affiliations appears at the end of the paper

Impaired gut barrier function may lead to progression of liver fibrosis in people with alcohol-related liver disease. The postbiotic ReFerm<sup>®</sup> can lower gut barrier permeability and may thereby reduce fibrosis formation. Here, we report the results from an open-labelled, single centre randomized controlled trial where 56 patients with advanced, compensated, alcohol-related liver disease were assigned 1:1 to receive either ReFerm<sup>®</sup> ( $n = 28$ ) or standard nutritional support (Fresubin<sup>®</sup>,  $n = 28$ ) for 24 weeks. The primary outcome was a  $\geq 10\%$  reduction of the fibrosis formation marker alpha-smooth muscle actin in liver biopsies, assessed by a blinded pathologist using automated digital imaging analysis. Paired liver biopsies meeting quality criteria for the primary outcome were available for 40 participants (ReFerm<sup>®</sup>,  $n = 21$  and Fresubin<sup>®</sup>,  $n = 19$ ). This reduction was observed in 29% of patients receiving ReFerm<sup>®</sup>, compared to 14% with Fresubin<sup>®</sup> (OR = 2.40; 95% CI 0.63 to 9.16;  $p = 0.200$ ). No treatment-related serious adverse events occurred. Our findings suggest that ReFerm<sup>®</sup> may reduce liver fibrosis by enhancing gut barrier function, potentially preventing the progression of alcohol-related liver disease.

Alcohol is the predominant cause of liver-related morbidity and mortality globally<sup>1</sup>. The selective gut barrier function is crucial for human health, while a reduced gut barrier is considered a main driver of liver fibrosis, leading to progression in alcohol-related liver disease (ALD)<sup>2,3</sup>. Activated hepatic stellate cells (HSCs) are key in the accumulation of collagen in the liver, which drives the development of fibrosis<sup>4,5</sup>. Immunohistochemical staining of liver biopsies for  $\alpha$ -smooth muscle actin ( $\alpha$ -SMA) is a marker of activated HSCs<sup>6,7</sup>.

Patients with advanced ALD have gut microbiome dysbiosis characterized by an altered composition and metabolism<sup>8</sup>. Such alteration of metabolism leads to a reduced production of beneficial short-chain fatty acids (SCFAs) and an increased production of harmful substances, which together impair the gut barrier<sup>8</sup>. The impaired gut barrier has increased permeability and allows the influx of harmful substances through the gut wall into the portal circulation<sup>8,9</sup>. Beyond

the inflammation induced by alcohol alone, the substances contribute to further inflammation in the liver, subsequently leading to fibrosis<sup>10</sup>. Therefore, therapeutic strategies that can halt this cascade by restoring the gut barrier may reduce liver fibrogenesis, leading to disease progression<sup>11,12</sup>. Postbiotics are defined as the preparation of inanimate microorganisms and/or their components that confer a health benefit on the host<sup>13</sup>. Consequently, postbiotics emerge as potential treatment options to restore the gut barrier and reduce liver fibrogenesis in ALD<sup>13,14</sup>. In this study, we investigate the efficacy of the postbiotic product ReFerm<sup>®</sup>, a food product of an oat gruel composition fermented with *Lactobacillus plantarum* DSM 9843, containing high amounts of microbial metabolites. ReFerm<sup>®</sup> has previously been shown to lower colonic barrier permeability<sup>15</sup> and to be efficacious for the treatment of active ulcerative colitis<sup>16</sup>. Furthermore, a recent animal study shows oat beta-glucan supplementation reduces liver

 e-mail: [Aleksander.Krag@rsyd.dk](mailto:Aleksander.Krag@rsyd.dk)

fibrosis development by reversing unfavorable changes in gut microbiota, resulting in an expansion of protective taxa, including *Lactobacillus*<sup>17</sup>. However, the efficacy of ReFerm® for halting liver fibrogenesis remains unknown.

In this work, we report the results from GALA-POSTBIO, a randomized controlled trial, where 56 patients were assigned 1:1 to receive either ReFerm® or standard nutritional support (Fresubin®) for 24 weeks. The primary endpoint was a post-treatment reduction of  $\geq 10\%$  of the fibrosis formation marker  $\alpha$ -SMA in liver biopsies. The primary outcome was reached in 29% of patients receiving ReFerm® and 14% with Fresubin®, but did not reach statistical significance. Secondary outcomes showed that treatment with ReFerm® was safe and improved markers of liver fibrogenesis (transient elastography (TE), enhanced liver fibrosis (ELF), and N-terminal type III collagen (PRO-C3)). The mode of action was explored with several omics techniques, showing that ReFerm® treatment was associated with improved gut barrier and hepatic regeneration as indicated by reduced levels of circulating intestinal fatty acids binding protein (I-FABP), and increased levels of Neurotrophin-3 (NT-3) and Sirtuin 2 (SIRT2). These findings were confirmed in an animal model.

## Results

### Patients

From March 8, 2019 to January 12, 2021, we screened 631 patients with advanced compensated liver disease and a history of excessive alcohol intake and identified 158 that fulfilled the inclusion criteria (Fig. 1). Hereof, 56 patients consented to participate and were randomly allocated to either ReFerm® ( $n = 28$ ) or Fresubin® ( $n = 28$ ), of which 41 of 56 (73%) completed the trial per-protocol (PP) (21 treated with ReFerm® and 20 treated with Fresubin®). Of those who completed the trial, 40 of 41 patients had paired liver biopsies meeting quality criteria for the assessment of the primary outcome. Conduction of the study was completed on August 12, 2021.

Baseline demographics and clinical characteristics were comparable between the patients allocated to treatment with ReFerm® and Fresubin® (Table 1). The median age was 63 (IQR 57–67) years, and 47 of 56 (84%) were males. Abstinence from alcohol 1 week prior to inclusion was reported by 14 of 28 (50%) in each group. In the PP population, the participants reporting abstinence 1 week prior to inclusion, 1 (2%) reported alcohol intake during the trial. Histological assessment showed that 48 of 56 (86%) had advanced fibrosis ( $\geq F3$ ), and the median liver stiffness using TE was 21 kPa (IQR 16–35).

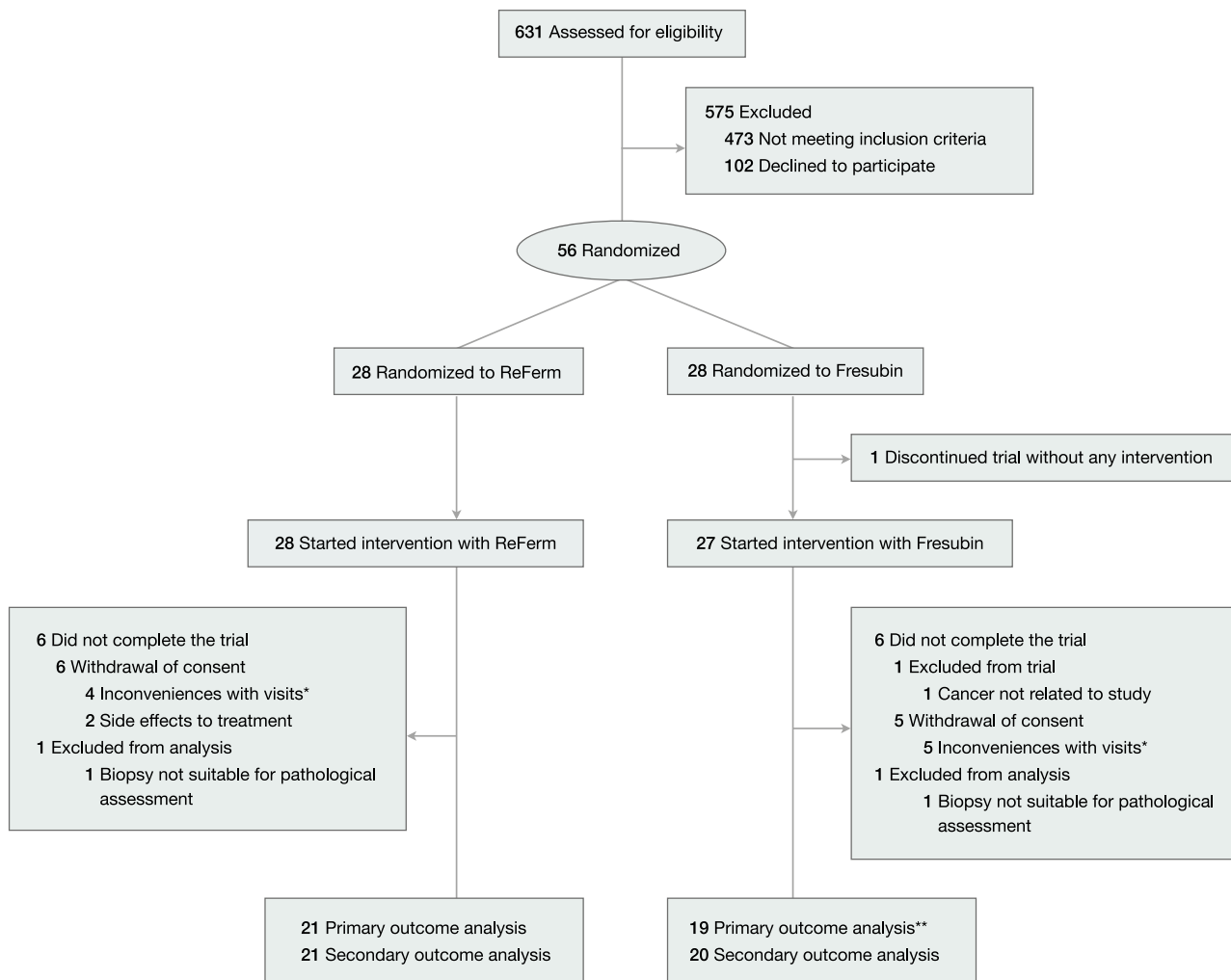


**Fig. 1 | GALA-POSTBIO trial flow chart.** The figure illustrates the process of patient inclusion, allocation, and evaluation throughout the trial. \*Four patients in allocated to ReFerm® treatment and five to Fresubin® did not complete the trial due to “inconvenience with visits,” which included a concern related to hospital visits during the COVID-19 pandemic. \*\*One patient allocated to Fresubin® treatment

completed the trial according to protocol, but the 24-week biopsy was not suitable for quantification of  $\alpha$ -SMA. Consequently, this patient was excluded from the primary endpoint analysis but included only in the secondary endpoint assessments.

**Table 1 | Demographic and baseline clinical characteristics**

	ReFerm® n = 28	Fresubin® n = 28
Age (IQR), years	62 (56–66)	64 (58–68)
Male sex, n	25 (89%)	22 (79%)
Body mass index $\geq$ 30 kg/m <sup>2</sup> , n	14 (50%)	11 (39%)
Type 2 diabetes, n	6 (21%)	3 (11%)
<b>Alcohol consumption</b>		
Abstinent $\geq$ 1 week prior to inclusion, n	14 (50%)	14 (50%)
Abstinent $\geq$ 1 year prior to inclusion, n <sup>a</sup>	7 (25%)	9 (32%)
Average alcohol intake for active drinkers (IQR), g/day	36 (14–60)	36 (9–51)
Phosphatidylethanol (IQR), $\mu$ /L <sup>a</sup>	0.16 (0.00–0.89)	0.20 (0.00–1.28)
<b>Laboratory data</b>		
Alanintransaminase (IQR), U/L	32 (20–50)	28 (22–52)
Aspartatransaminase (IQR), U/L	43 (26–78)	36 (26–53)
Gamma-Glutamyltransferase (IQR), U/L	163 (69–411)	132 (66–465)
Bilirubin, (IQR), $\mu$ mol/L	12 (10–20)	12 (7–18)
Platelets (SD), 10 <sup>9</sup> /L	164 (69)	164 (44)
INR (SD)	1.15 (0.13)	1.14 (0.17)
Albumin (SD), g/L	44 (4)	44 (3)
C-reactive protein (IQR), mg/L	2 (1–4)	2 (1–4)
MELD-Na (IQR)	9 (8–11)	10 (8–12)
Child-Pugh class A, n	28 (100%)	28 (100%)
<b>Liver histology</b>		
$\alpha$ -SMA (IQR) <sup>b</sup>	21.9 (17.7–38.7)	19.7 (11.7–26.8)
Kleiner fibrosis stage 2/3/4, n	2/6/18	2/9/15
Lobular inflammation grade 0/1/2/3, n	6/14/6/0	7/17/2/0
Ballooning grade 0/1/2, n	16/10/0	15/11/0
Steatosis grade 0/1/2/3, n	13/8/3/2	7/8/9/2
<b>Non-invasive test of liver disease</b>		
TE (IQR), kPa	27.5 (16.5–46.2)	20.2 (13.4–27.0)
CAP (IQR), dB/m	298.5 (240.0–335.0)	304.5 (262.0–336.0)
2D-SWE (SD), kPa	23 (13)	22 (12)
PRO-C3 (SD), ng/mL	27.0 (10.5)	23.0 (7.2)
Enhanced Liver Fibrosis test (SD) <sup>c</sup>	10.8 (1.0)	10.5 (0.9)
Fibrosis-4 score (IQR) <sup>c</sup>	2.8 (1.8–4.3)	2.7 (1.8–4.4)

Normally distributed data are presented as mean (SD), non-normally distributed data as median (IQR), and categorical data as counts (proportion, %). The sum of percentages may deviate from 100 due to rounding.

INR international normalized ratio, MELD-Na model for end-stage liver disease sodium,  $\alpha$ -SMA  $\alpha$  smooth muscle actin activation, TE Transient Elastography, CAP Controlled Attenuation Parameter, 2D-SWE two-dimensional shear wave elastography, PRO-C3 fragment of N-terminal type III collagen.

<sup>a</sup>Based on 49 patients.

<sup>b</sup>Based on 40 patients.

<sup>c</sup>Based on 46 patients.

In the PP population, the median compliance was 92% (IQR 77–98) for patients treated with ReFerm® and 99% (IQR 94–100) for patients treated with Fresubin®. During the trial, the self-reported alcohol intake was comparable between the groups, with a median alcohol

intake of 32 (IQR 24–39) g/day (Fig. S1A). PEth measured at baseline, 4 weeks, and 24 weeks were also comparable between groups (Table S1).

### Efficacy of intervention

In the primary outcome PP analysis, 8 of 21 (38%) patients treated with ReFerm® achieved a  $\geq$ 10% reduction in  $\alpha$ -SMA expression compared to 4 of 19 (21%) patients treated with Fresubin® (OR = 2.31; 95% CI: 0.56–9.47;  $p$  = 0.246) (Fig. 2A). The results were consistent in the intention-to-treat (ITT) analysis showing 8 of 28 (29%) treated with ReFerm® achieved a  $\geq$ 10% reduction in  $\alpha$ -SMA expression compared with 4 of 28 (14%) treated with Fresubin® (OR = 2.40; 95% CI: 0.63–9.16;  $p$  = 0.200). We performed a post-hoc sensitivity analysis to investigate the impact of treatment compliance. The analysis showed that increasing compliance correlated with a reduction in the  $\alpha$ -SMA expression in patients treated with ReFerm® but not Fresubin® (Spearman correlations; ReFerm®,  $Rho$  = -0.6623;  $p$  = 0.0011; Fresubin® group,  $Rho$  = 0.0335;  $p$  = 0.8918) (Fig. 2C, D). Adjusted for treatment compliance, patients treated with ReFerm® achieved a mean reduction of  $\alpha$ -SMA expression by -8.3% compared to Fresubin® (-7.7% vs. 0.6%,  $p$  = 0.012) (Fig. 2E).

Secondary outcome showed changes in non-invasive markers from baseline to end-of-treatment in the PP population are shown in Fig. 2B, F. Notably, a clinically significant reduction ( $\geq$ 20%) in liver stiffness by TE was achieved in 8 of 21 (38%) of patients treated with ReFerm® and 2 of 20 (10%) treated with Fresubin® (OR = 5.54, 95%CI 1.01–30.5,  $p$  = 0.049) (Figs. 2B and S2). Furthermore, the fibroblast activity marker PRO-C3 decreased by 14% in patients treated with ReFerm® compared to Fresubin® (-1.91 (-7%) vs. 1.60 ng/mL (+7%),  $p$  = 0.062).

Histological improvement, defined as a reduction in Kleiner fibrosis stage, was seen in 6 of 21 (29%) patients treated with ReFerm® and 3 of 20 (15%) treated with Fresubin® (OR = 2.2; 95% CI: 0.48–10.68,  $p$  = 0.301) (Fig. S3). Individual histological features of steatohepatitis (lobular inflammation, hepatocyte ballooning, and steatosis) did not show significant differences between the groups, but worsening of lobular inflammation was seen in 1 of 21 (5%) treated with ReFerm® group compared to the 5 of 20 (25%) treated with Fresubin® ( $p$  = 0.098) (Fig. S3).

We conducted a subgroup analysis to assess the impact of alcohol abstinence. Among the participants who completed the study, 17 self-reported maintaining abstinence throughout the study: 8 in the ReFerm® group and 9 in the Fresubin® group. Of these 17 participants, 11 had PEth measurements consistently below 0.05  $\mu$ mol/L at baseline, 4 weeks, and after 24 weeks of treatment, with 4 in the ReFerm® group and 7 in the Fresubin® group. There was a higher proportion of participants with both low and high PEth values achieving the primary endpoint in the group treated with ReFerm® compared to Fresubin®, although this difference was not statistically significant (Table S2). It is well established that alcohol consumption impacts the prognosis of ALD<sup>18</sup>. This subgroup analysis suggests that the effect of ReFerm® on  $\alpha$ -SMA was not mediated by lower alcohol intake.

### Safety

No serious adverse events related to the treatment occurred during the trial. In the ReFerm® group, 27 of 28 (96%) patients reported at least one adverse event compared to 26 of 28 (93%) in the Fresubin® group ( $p$  = 0.550). In general, adverse events were considered mild, and each type was equally reported between groups (Table S3).

### Mechanistic exploration of ReFerm® treatment

This section explores the treatment effect of ReFerm® on the gut-liver axis with several omics techniques. Significant findings are integrated to link clinical impact on the dynamics of the gut-liver axis to understand the mode of action.

**Minimally impacts on microbiome composition, but alteration of key pathways**

We analyzed fecal samples at four time points from the 41 patients who had completed the trial PP. The four time points were at baseline, after

4 weeks and 24 weeks of treatment, and 6–8 weeks after ending the treatment.

Here we detected 1276 species, of which 312 were detected in more than 20% of the samples. When comparing changes from

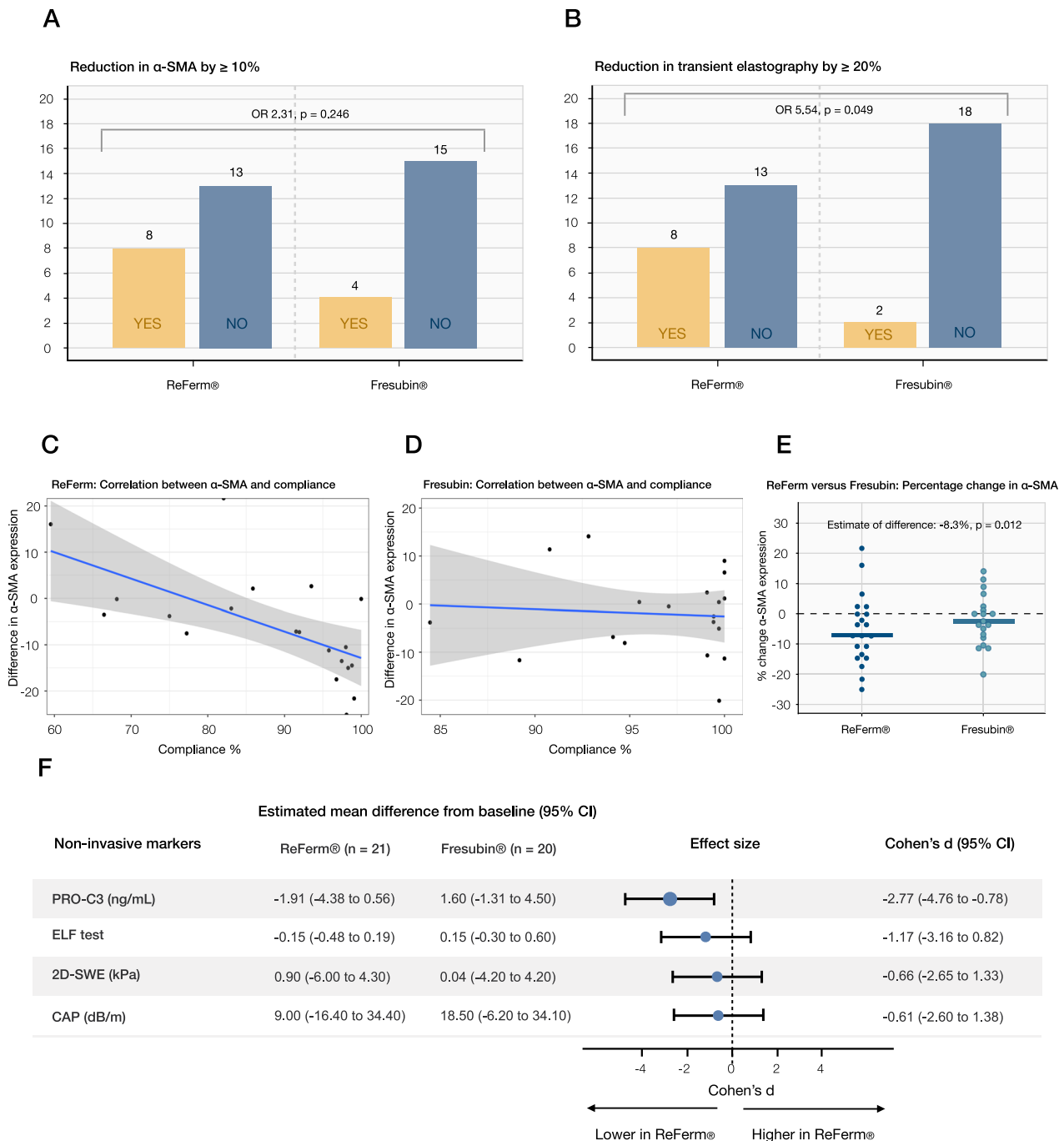
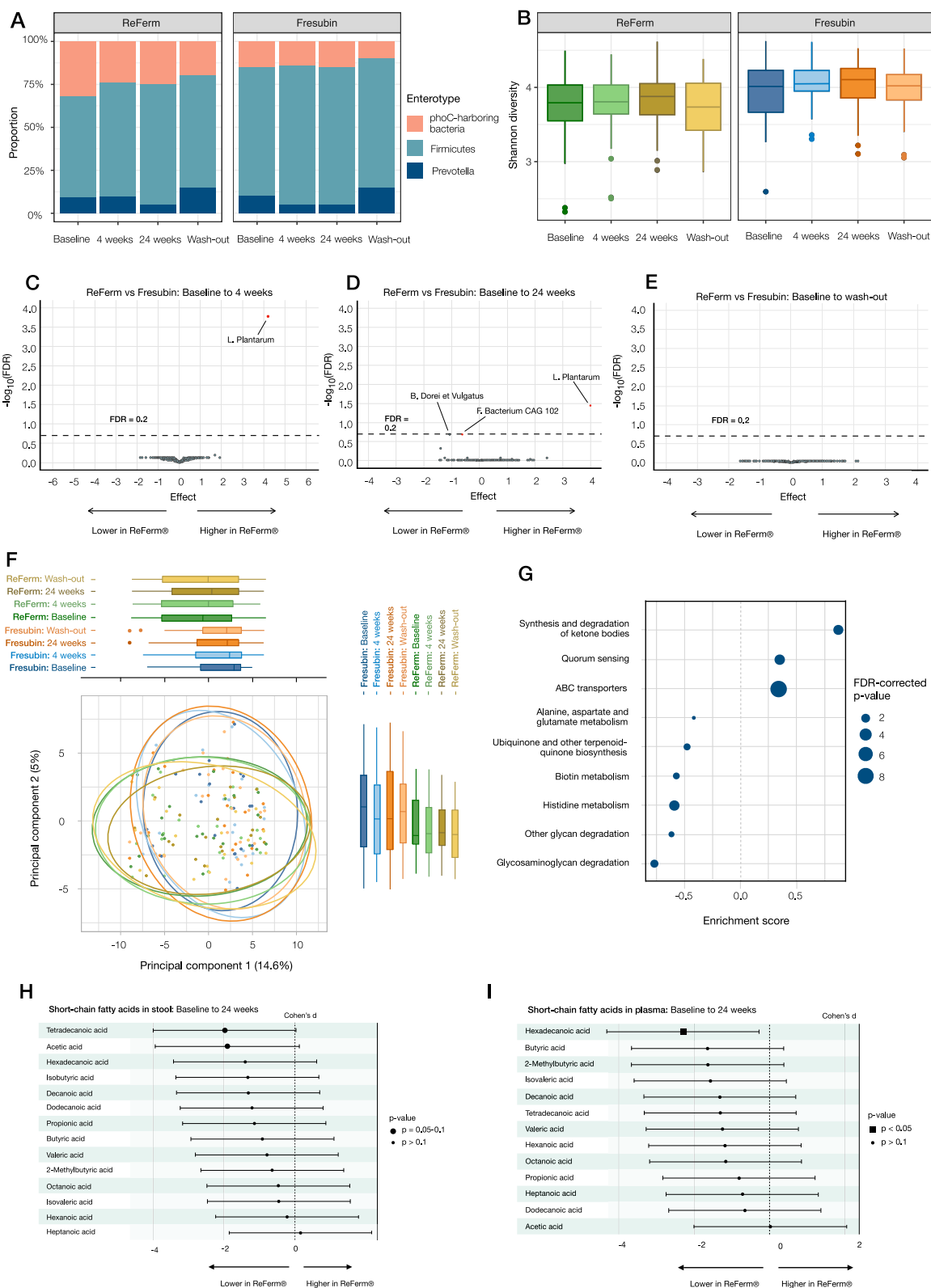


**Fig. 2 | Treatment effect on clinical outcomes for the per-protocol population.**

**A** Bar chart of the number of patients having at least 10% reduction in  $\alpha$ -SMA expression (primary endpoint), yellow = Yes, blue = No. **B** Bar chart of the number of patients having at least 20% reduction in liver stiffness measured by transient elastography, yellow = Yes, blue = No. **C, D** Scatter plots of treatment effect and compliance for each treatment group. Error bands = 95% confidence intervals. Treatment effect was estimated as percentage change in  $\alpha$ -SMA expression from baseline to 24 weeks,  $n = 40$ . **E** Dot plot showing percentage change in  $\alpha$ -SMA expression from baseline to 24 weeks,  $n = 40$  ( $p$  value derived from estimation adjusted for compliance). **F** Estimated mean difference (95% confidence intervals)

of non-invasive tests combined with a forest plot of Cohen's  $d$  to compare effect size. Forest plot of effect sizes and corresponding 95% confidence intervals for changes in non-invasive secondary endpoints between baseline and 24 weeks, PRO-C3  $n = 40$ , ELF test  $n = 40$ , 2D-SWE  $n = 38$ , CAP  $n = 41$ . All  $p$  values are two-sided. **A, B** Odds ratios (OR) were calculated using unadjusted logistic regression. **E** The estimate of difference was calculated using linear regression, adjusted for compliance.  $\alpha$ -SMA Alpha Smooth Muscle Actin, TE transient elastography, ELF test enhanced liver fibrosis test, PRO-C3 fragment of N-terminal type III collagen, SWE shear wave elastography, CAP controlled attenuation parameter. Source data are provided as a Source Data file.



baseline throughout the trial, the enterotype proportion, Shannon diversity remained stable for both groups (Fig. 3A, B). However, a notable improvement in dysbiosis was observed in patients treated with ReFerm<sup>®</sup> after 24 weeks, though it was not statistically significant (Fig. S4). At the species level, *L. plantarum* significantly increased from baseline to 4 and 24 weeks of treatment in patients treated with ReFerm<sup>®</sup> compared to Fresubin<sup>®</sup> (FDR < 0.2) (Fig. 3C, D). In samples

collected 6–8 weeks after end-of-treatment, *L. plantarum* was no longer increased in the ReFerm<sup>®</sup> group compared to the Fresubin<sup>®</sup> group (Fig. 3E). Apart from *L. plantarum*, no changes at the species level passed the significance threshold after correction for multiple testing (Fig. 3C–E) and the composition remained stable throughout the trial in both groups (Fig. 3F). The pathway enrichment analysis of the ReFerm<sup>®</sup> group from baseline until 24 weeks of treatment

**Fig. 3 | Treatment effect on the gut microbiome.** **A, B** Proportions of the fecal bacterial composition (enterotype level, dark blue = Prevotella, light blue = Firmicutes, pink = Bacteroides/Phocaeicola) and diversity (Shannon diversity) at baseline (dark green,  $n = 41$ ), after 4 weeks (light green,  $n = 42$ ) and 24 weeks of treatment (brown,  $n = 40$ ) and after a “wash-out” period 6–8 weeks after last day of treatment (yellow,  $n = 40$ ). **C–E** Volcano plots of changes in the abundance of microbial species at the strain level during the trial. Changes are calculated as changes between the groups from baseline to the specific time points. **F** Principal component plot of the gut microbiome composition during the trial showing minimal changes within each treatment group, dark blue = Fresubin® baseline ( $n = 20$ ), light blue = Fresubin® 4 weeks ( $n = 21$ ), dark orange = Fresubin® 24 weeks ( $n = 20$ ), light orange = Fresubin® after washout ( $n = 20$ ), dark green = ReFerm® baseline ( $n = 22$ ), light green = ReFerm® 4 weeks ( $n = 21$ ), brown = ReFerm® 24 weeks ( $n = 20$ ), yellow = ReFerm® after washout ( $n = 20$ ). **G** Pathway enrichment analysis of gut microbial pathways that significantly change in the group treated

with ReFerm® from baseline to 24 weeks. The analysis was performed using the GSEA function in the clusterprofiler package, which applies a one-sided test to assess whether pathways are significantly enriched in either direction. Cohen's  $d$  effect sizes were used as the ranking metric for each feature. KEGG pathways with  $p$  values of  $<0.1$  before correction for multiple testing are shown. **H, I** Forest plot of Cohen's  $d$  estimates of changes in short-chain fatty acid levels in stool ( $n = 38$ ) and plasma ( $n = 39$ ) from baseline to 24 weeks. Estimates were derived from a within-group analysis and were estimated using a general linear model, with Cohen's  $d$  used to standardize effect sizes. Adjustments for multiple testing were applied, and error bars represent 95% confidence intervals. Box plots show the distribution of data with the center line representing the median (50th percentile). The box bounds indicate the interquartile range (IQR; 25th to 75th percentile), while the whiskers extend to the smallest and largest values within  $1.5 \times$  IQR. Data points beyond the whiskers are plotted as outliers. Source data are provided as a Source Data file.

demonstrated that nine biological pathways were significantly changed (Fig. 3G). The observed changes, including a reduction in glycan degradation and an increase in turnover of ketone bodies, histidine, and biotin, indicate a change in the overall gut microbiome metabolism (Fig. 3G). The relative levels of SCFAs were measured in both stool and circulation at baseline and after 24 weeks of treatment. Compared to baseline, patients treated with ReFerm® decreased relatively more in SCFAs, including butyric and propionic acid (Fig. 3H, I). Hexadecenoic acid decreased in both stool and plasma, and acetic acid had the highest variation, with a decrease in stool and was stable in plasma.

### Reduces gut barrier dysfunction and increases hepatic regeneration

A panel of 184 proteins was measured from baseline and after 24 weeks of treatment. Hereof, quality control (QC) was passed by 165 proteins from 37 patients (ReFerm®,  $n = 18$  and Fresubin®,  $n = 19$ ) with both measurements from baseline and after 24 weeks. Changes from baseline to 24 weeks of treatment were compared between patients treated with ReFerm® and Fresubin® (Fig. 4A). We identified five proteins that changed significantly after 24 weeks of treatment ( $p < 0.05$ , Fig. 4A–C). Of these five proteins, the gut barrier impairment marker I-FABP decreased in patients treated with ReFerm® compared to Fresubin® (Fig. 4B). Furthermore, the analysis showed an increase in the hepatic regeneration marker Neurotrophin-3 (NT-3) and Sirtuin 2 (SIRT2). Significant decrease of interleukin-17A (IL-17A) serum levels and increase of Leptin serum levels were observed in patients treated with Fresubin® while levels remained stable in patients treated with ReFerm® (Fig. 4B). ReFerm® has a minor impact on hepatic synthesis and excretion function (Figs. S5 and S6).

### Relationship between clinical and molecular effects of ReFerm®

The association between changes in the primary outcome ( $\alpha$ -SMA) and the selected significant features detected from the omics analyses was explored in a combined analysis of  $\alpha$ -SMA, *Lactobacillus plantarum*, and cytokines I-FABP, SIRT2, and NT-3 (Fig. 4D). This analysis showed that a reduction of  $\alpha$ -SMA was correlated with a reduction in I-FABP ( $\rho: 0.27$ ) and an increase of SIRT2 ( $\rho: 0.34$ ), *L. plantarum* ( $\rho: 0.23$ ), and hepatic regeneration (NT-3  $\rho: 0.14$ ). Furthermore, the analysis showed that high levels of *L. plantarum*, as a marker for treatment with ReFerm®, were correlated with a reduction in I-FABP ( $\rho: -0.17$ ), together with an increase of NT-3 ( $\rho: 0.48$ ) and SIRT2 ( $\rho: 0.37$ ).

### Validation of key findings in animal models

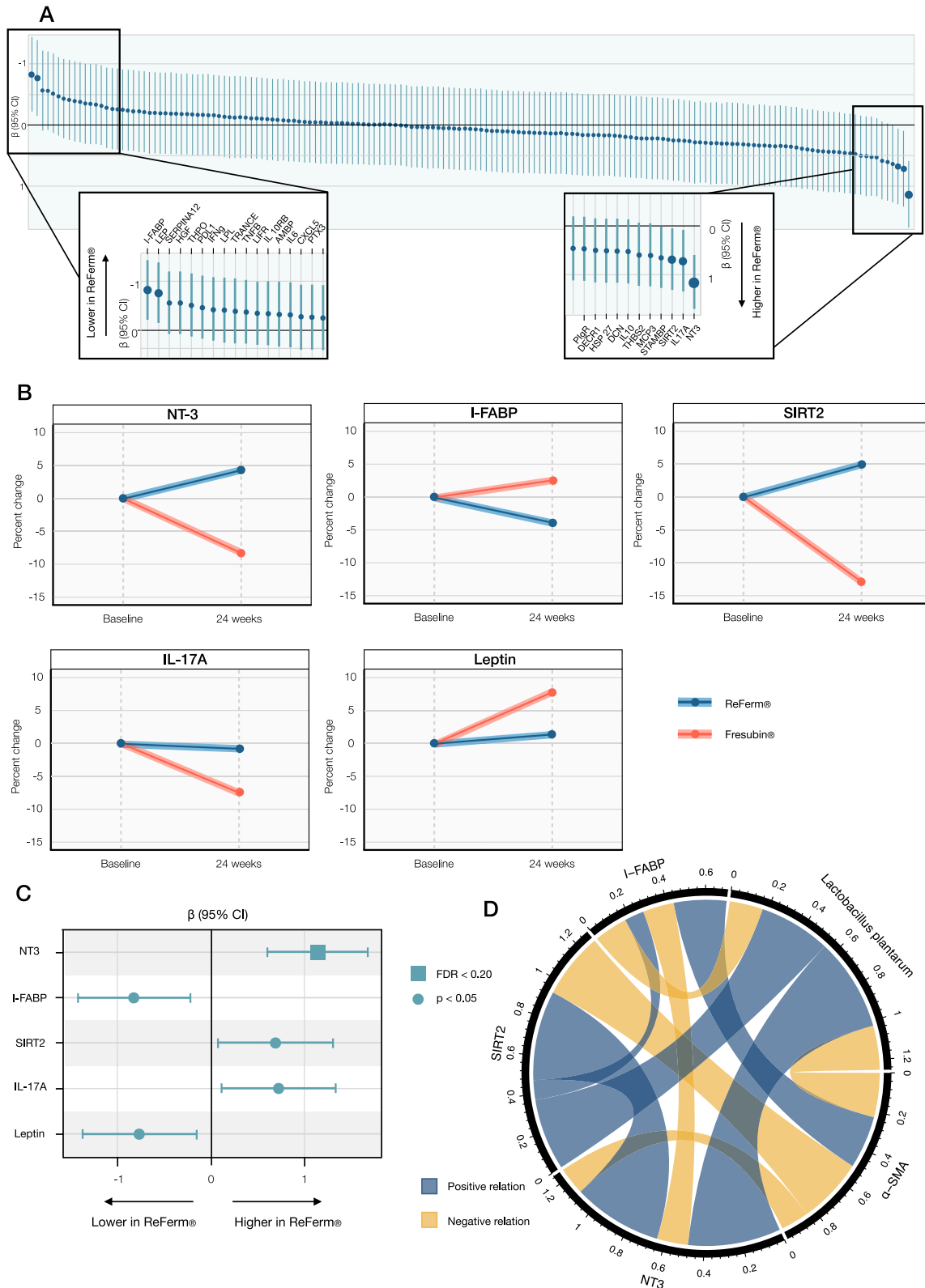
In order to explore the proposed mode of action in an animal model, ReFerm® and Fresubin® were applied in an animal model of ALD (Fig. S8). In this model, 11 specific pathogen-free male wild-type mice, aged 12 weeks, had induced ALD. The intervention groups received twice daily oral gavage (0.3 ml) of Fresubin® ( $N = 4$ ) or ReFerm® ( $N = 3$ )

for 1 week prior to sacrifice, while an ALD control group remained untreated ( $N = 4$ ). Age-matched, untreated mice served as controls for all experiments ( $N = 3$ ). On the gene expression level, induction of ALD led to an increase in liver Collagen 1 (Col1A1,  $p = 0.053$ ) that was ameliorated by ReFerm® treatment ( $p = 0.079$  for ALD with and without ReFerm®). Compared to untreated controls, ReFerm® treatment also led to a decrease in  $\alpha$ -SMA ( $p = 0.046$ ). These changes suggest less activation of HSCs and decreased collagen production (Fig. S9A). In the gut, an increase of gut barrier integrity was demonstrated through elevated mRNA levels of vinculin in the jejunum ( $p = 0.07$  for ALD with and without ReFerm®, Fig. S9B). I-FABP and SIRT2 protein levels were increased in the ALD group compared to control mice. However, no significant changes could be observed for I-FABP and SIRT2 protein levels (Fig. S9C). In conclusion, this small-scale exploration on the effects of ReFerm® in an animal model shows a similar response to treatment in humans and mice.

## Discussion

In the 24-week GALA-POSTBIO trial, an investigator-initiated, randomized, open-label active-comparator trial of patients with advanced ALD treated with ReFerm® or Fresubin®, there was no significant difference in achieving the primary endpoint (a  $\geq 10\%$  reduction in  $\alpha$ -SMA expression). However, in those with high compliance to treatment, patients treated with ReFerm® experienced an 8% reduction in  $\alpha$ -SMA expression compared to Fresubin®. This beneficial effect was supported by a significantly higher proportion achieving a clinically significant reduction ( $\geq 20\%$ ) in liver stiffness, which has recently been validated as a marker of improved prognosis in ALD<sup>19</sup>. Furthermore, a corresponding decrease in the collagen formation biomarker PRO-C3 was seen in patients treated with ReFerm®. The exploratory mechanistic multi-omics analysis showed that the beneficial effect of ReFerm® seems to be mediated through enhancement of the gut barrier, leading to hepatic regeneration without changing the microbiome composition and not affecting immunity.

ALD, the leading cause of liver-related mortality in the USA<sup>20</sup> and Europe<sup>1</sup>, is associated with microbiome dysbiosis<sup>21,22</sup> and impaired gut barrier<sup>23,24</sup> that are considered key drivers of the disease process and promising therapeutic targets. In the GALA-POSTBIO trial, we investigated the effect of ReFerm® on patients with advanced ALD. ReFerm® is a postbiotic previously demonstrated to improve colonic barrier function by increasing transepithelial resistance in patients with irritable bowel syndrome<sup>15</sup>. Our study shows that ReFerm® decreased blood levels of I-FABP, a marker expressed in the epithelial cells and released into the circulation when the gut epithelia are disrupted<sup>25,26</sup>. A cross-sectional study of patients with liver disease demonstrated a stepwise increase in plasma concentrations of I-FABP from healthy controls over compensated cirrhosis to the highest levels in decompensated cirrhosis<sup>27</sup>. It is therefore noteworthy that our study showed that a decrease in I-FABP levels was correlated with a reduction of  $\alpha$ -



SMA. This finding supports that an intervention that reduces gut barrier impairment is directly linked to halting fibrosis formation in patients with advanced ALD (Fig. 5). Moreover, our study indicates that modification of the microbiome composition may not be essential for therapeutic efficacy. This inference is reinforced by earlier studies demonstrating that Rifaximin enhances gut barrier function with only a minor impact on gut microbiome composition<sup>28</sup>, while we have

previously reported that Rifaximin seems to prevent the progression of liver fibrosis<sup>29</sup>. Consequently, it is noteworthy that our study demonstrates the direct connection between the gut barrier and markers of liver fibrosis formation.

In our study, treatment with ReFerm® led to a reduction in several markers of fibrosis formation. Lower  $\alpha$ -SMA expression suggests a reduced activity of HSCs, closely linked to fibrosis formation<sup>30–32</sup>.

**Fig. 4 | The effect on plasma proteins.** **A** Forest plot of changes of all measured proteins from baseline to 24 weeks compared between patients treated with ReFerm® ( $n = 21$ ) and Fresubin® ( $n = 20$ ). Selected proteins showing the largest changes ( $\beta$ -coefficient) are highlighted. The estimated shown are  $\beta$ -effects (95% confidence intervals) per 1-SD change in plasma protein levels. **B** Line plot of percent change in levels of five selected proteins from baseline to 24 weeks. Blue = ReFerm® ( $n = 21$ ), red = Fresubin® ( $n = 20$ ). **C** Forest plot of the five selected proteins showing  $\beta$ -effects. Estimates were derived from a within-group analysis (ReFerm®,  $n = 21$ ) and were estimated using a general linear model, with Cohen's  $d$  used to

standardize effect sizes. Adjustments for multiple testing were applied. Data points represent the mean with 95% confidence intervals. **D** Circos plot of associations between key features affected in patients treated with ReFerm®. "Positive relation," blue, indicates that as one feature increases, the correlated feature similarly increases. "Negative relation," yellow, indicates that as one feature increases, the correlated feature decreases and vice versa.  $\alpha$ -SMA Alpha Smooth Muscle Actin, IL-17A interleukin-17A, LEP leptin, I-FABP intestinal fatty acid-binding protein, NT-3 neurotrophin-3, SIRT2 NAD-dependent protein deacetylase Sirtuin 2. Source data are provided as a Source Data file.

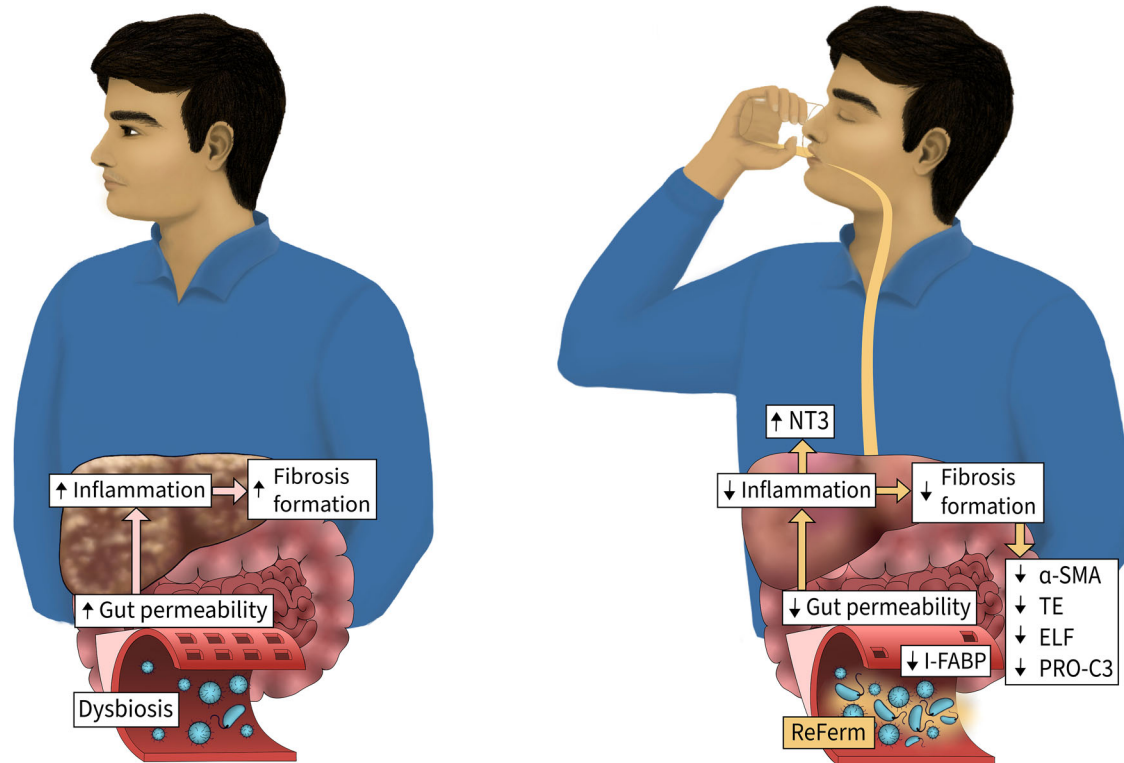


**Fig. 5 | Mode of action.** In alcohol-related liver disease progression of liver fibrosis is driven by gut dysbiosis and increased gut permeability, leading to a translocation of bacterial products to the liver, inducing inflammation and fibrosis formation. Treatment with ReFerm® leads to an improved gut barrier (reduction in gut permeability) marked by reduced levels of circulating intestinal fatty acid-binding protein (I-FABP). The improved gut barrier leads to a decrease in liver inflammation

and induction of hepatic regeneration marked by higher levels of circulating Neurotrophin-3 (NT-3), which leads to lower fibrosis formation marked by improvement (reduction) in  $\alpha$ -smooth muscle actin ( $\alpha$ -SMA), transient elastography (TE), enhanced liver fibrosis (ELF), and N-terminal type III collagen (PRO-C3).

An analysis of two RCTs involving 1,135 patients with MASH and cirrhosis showed that  $\alpha$ -SMA decreased by  $-6\%$  in those who experienced cirrhosis regression, compared to an increase of  $+0.6\%$  in those who did not experience cirrhosis regression<sup>33</sup>. Conversely, an increase in  $\alpha$ -SMA from baseline was associated with liver-related events (HR 1.18, 95% CI: 1.05–1.32). A similar decline was observed in PRO-C3 levels, a circulating collagen formation marker associated with higher risks of hepatic decompensation<sup>34</sup>. Moreover, the proportion of patients achieving a clinically significant reduction ( $>20\%$ ) in liver stiffness measurement (LSM), which is correlated with a reduced risk of hepatic decompensation<sup>35</sup>, was significantly higher in patients treated with ReFerm® than with Fresubin®. On top of this, the reduction of gut barrier impairment marker I-FABP was associated with an increase in levels of NT-3 that is considered to promote hepatocyte proliferation, leading to liver regeneration<sup>36,37</sup> and increased levels of SIRT2, potentially preventive for ethanol-induced liver injury<sup>38</sup>. These results suggest a potential for hepatic recovery when arresting disease progression. IL-17A is important for neutrophil recruitment and augmentation of antibacterial responses to pathogenic bacteria and has

been found to increase in patients with hepatic encephalopathy treated with Rifaximin<sup>39,40</sup>. In the ReFerm® group, we observed stability in IL-17A levels, whereas there was a decrease in the Fresubin® group. Leptin is known to promote inflammation<sup>41</sup>. In the ReFerm® group, leptin levels remained stable, while the Fresubin® group experienced an increase. These results suggest a deterioration in inflammation in the Fresubin® group while stable in the ReFerm® group. This trend was confirmed in the proof-of-concept animal model, where we also identified signals indicating enhanced gut barrier function, along with reduced  $\alpha$ -SMA in the liver and combined decreased systemic inflammation.

A postbiotic is defined as a preparation of inanimate microorganisms and/or their components that confers a health benefit on the host<sup>13</sup>. In contrast, a probiotic is defined as a product with living microorganisms that confer a health benefit on the host<sup>13</sup>. In this study, the formulation of ReFerm® contained both *Lactobacillus plantarum* DSM 9843 and its fermentation products of microbial metabolites, including SCFAs. We employed shotgun metagenomic analysis for microbiome composition assessment, showing a significant increase

of *Lactobacillus plantarum* DSM 9843 in stool samples from patients treated with ReFerm<sup>®</sup>, but this method does not differentiate between viable and non-viable microorganisms. However, in vitro experiments on CACO-2 cells exposed to ReFerm<sup>®</sup> with heat-inactivated *Lactobacillus plantarum* DSM 9843 indicate that the improvement of the epithelial barrier function is not attributed to live *Lactobacillus plantarum* DSM 9843 but rather to microbial metabolites and/or cell components. Additionally, a previous randomized controlled trial of patients with stable cirrhosis showed that live *Lactobacillus casei* did not reduce the risk of infection or hepatic decompensation<sup>42</sup>, suggesting that the postbiotic component of ReFerm<sup>®</sup> might likely be responsible for the observed effects on gut barrier integrity and the subsequent halting of fibrosis formation.

This study has limitations. First, we applied a trial design using Fresubin<sup>®</sup> as an active comparator, which is a product used for general nutritional support in patients with liver disease in Denmark. The rationale for using an active comparator was that many patients with advanced liver disease have compromised nutritional status, and consequently, nutritional support in general improves outcome<sup>43,44</sup>. Therefore, it appears plausible that treatment with Fresubin<sup>®</sup> may have been beneficial for the patients. Consequently, the therapeutic effects of ReFerm<sup>®</sup> should be interpreted as improvements beyond the baseline improvements attributed to general nutritional support. Second, a double-blind treatment approach was unfeasible given that many patients with liver disease are familiar with the taste of Fresubin<sup>®</sup>, while ReFerm<sup>®</sup> possesses a distinct fermented sensory nature and taste. This limitation might have influenced participant behavior. To address this concern, we compared dropout rates and patient characteristics across both intervention groups, which were found to be comparable. Furthermore, we applied blinded outcome assessments to reduce the potential information bias associated with open-label trials. Third, this study design included patients with ALD ranging from significant fibrosis (F2) to compensated cirrhosis (F4), as regression is considered achievable across this spectrum of liver fibrosis<sup>45</sup>. There may likely be a biological difference in the ability for fibrosis regression depending on the severity of fibrosis, which may have led to a heterogeneous effect of the interventions and could potentially limit the generalizability to people with less severe liver fibrosis. Although patients were randomly allocated, there was an observed higher baseline LSM in the ReFerm<sup>®</sup> group compared to the Fresubin<sup>®</sup> group. This discrepancy may influence the interpretation of liver stiffness changes over time. However, histology and other non-invasive tests, such as the ELF score and FIB-4, were more consistent between the groups at baseline, suggesting that the overall liver fibrosis stage was comparable. Furthermore, this study included mainly men in the 50s and 60s, which may limit the generalizability of the results to younger patients, including women. Notably,  $\alpha$ -SMA expression, the primary endpoint, showed a significant decrease when adjusting for compliance, indicating that sufficient intake of the intervention product is necessary for efficacy. However, alternative explanations cannot be excluded. The most plausible alternative is that non-compliance may have been associated with higher alcohol consumption, potentially explaining the lack of effect. Nevertheless, subgroup analyses confirmed that the effect of ReFerm<sup>®</sup> on  $\alpha$ -SMA was not driven by reduced alcohol intake. Fourth, for omics analysis, we applied a false discovery rate (FDR) < 0.2 for multiple testing correction, which is higher than the threshold typically used in omics studies. We decided to apply this less strict threshold due to the trial cohort size. This approach was essential to balance the risk of missing important data against the likelihood of false positives in our exploratory study. Consequently, there is an increased risk that random features from these analyses have come out significant due to the relaxed threshold. It is important to consider that the most prominent findings, specifically the alterations in I-FABP, NT-3, and *Lactobacillus plantarum* DSM 9843, are of substantial biological relevance. Their direct relation to the hypothesis

of the study supports that these findings are not merely random but reflect biologically meaningful changes. Lastly, the small sample size in the animal model may limit the robustness of the findings, and a larger dataset is required could further elucidate the underlying mode of action.

It should be noted that the design and execution of this study were completed prior to the introduction of the SLD nomenclature<sup>46</sup>. At inclusion, nearly all participants exhibited at least one cardiometabolic factor, and 50% reported being alcohol abstinent. These individuals could technically be classified as MASLD according to the SLD nomenclature<sup>46</sup>, as the SLD classification does not account for past alcohol use or potential future increases in consumption<sup>47</sup>. However, over 50% of individuals with a history of high alcohol intake, who are classified as MASLD according to the SLD nomenclature, subsequently increase their consumption to levels consistent with MetALD/ALD<sup>47</sup>. We therefore chose to label this as a study of patients with ALD.

In patients with advanced ALD, 24 weeks of treatment with the postbiotic ReFerm<sup>®</sup> may reduce activated HSCs by enhancing gut barrier function, thereby potentially preventing progression of ALD. These findings support that treatments improving the gut barrier can be used to treat patients with ALD. However, this needs to be confirmed in larger trials with clinical endpoints.

## Methods

### Trial design

GALA-POSTBIO was a 24-week investigator-initiated, randomized, open-label active-comparator-controlled phase 2 trial investigating the efficacy of the postbiotic ReFerm<sup>®</sup> on liver fibrogenesis in patients with advanced ALD. The trial was approved by the Danish Data Protection Agency (19/6646) and the Ethical Committees of the Region of Southern Denmark (S-20170163) and followed the Helsinki Declaration. Patients provided written informed consent, and the trial is registered on [www.clinicaltrials.gov](http://www.clinicaltrials.gov) (<https://clinicaltrials.gov/study/NCT03863730?term=NCT03863730&rank=1>, NCT03863730), adhering to CONSORT guidelines. The full protocol is available in the Supplementary Materials. All authors had access to the study data and reviewed and approved the final manuscript.

The study design was presented to and reviewed by our Patient and Public Involvement board, ensuring that the patient perspectives were integrated. The board continues to be involved in dissemination plans for this research.

The intervention product in this manuscript is called ReFerm<sup>®</sup>, while in previous studies<sup>16,48</sup> and in the protocol, it was referred to as Profermin<sup>®</sup>. In June 2022, the company changed the name of the intervention product, but the product composition remains the same. Similarly, the bacterial name reported as part of the intervention product is labeled *Lactobacillus plantarum* DSM 9843, whereas in the protocol, it appears as *Lactobacillus plantarum* 299v<sup>®</sup> (Brand name owned by Probi AB, Sweden). The product remains the same, and the change has only been made for proprietary reasons.

As planned in the study protocol, we were originally going to analyze hepatic venous pressure gradient and liver vein outflow of microbial products. However, due to the low number of participants with data from liver vein catheterization, we did not have sufficient power to analyze these aspects. Although measurement of collagen proportionate area (%), circulating  $\alpha$ -SMA concentration, and degradation products M30 and M65 was initially included in our study protocol, we were unable to perform these analyses due to funding limitations. Given the extensive scope of the analyses already included in the study, resources had to be prioritized, and these specific biomarker assays were ultimately not feasible within the available budget. Similarly, other planned assessments, including the Forns index, APRI score, FIB-4, metabolic parameters, and ultrasonographic steatosis evaluation, were omitted from the final report due to space limitations and to maintain focus on the most pertinent findings.

## Patients

We identified potential participants at gastroenterology and hepatology departments across the Region of Southern Denmark, and all investigations were conducted at Odense University Hospital (Odense, Denmark). Eligible patients were aged 30–75 with advanced compensated ALD. Advanced ALD was defined as either liver stiffness by TE  $\geq 15$  kPa, a liver biopsy within the last 6 months showing fibrosis stage  $\geq 3$ , or a liver biopsy more than 6 months old showing fibrosis stage  $\geq 3$  and current liver stiffness  $\geq 10$  kPa. We considered excessive alcohol intake as the etiology if there was a history of excessive alcohol consumption, averaging at least 24 g/day for women and 36 g/day for men, sustained for a minimum of 5 years without any other known liver disease. Additional inclusion criteria included the ability to understand and speak Danish, both written and spoken, and the provision of informed consent. The presence of cardiometabolic risk factors at the time of inclusion was permitted. To ensure inclusion of only participants with compensated liver disease we excluded participants who had been hospitalized within 3 months of inclusion or who had moderate or severe ascites determined from imaging diagnostic, high-risk varices requiring intervention, Child-Pugh score of C, or a model for end-stage liver disease–Na (MELD–Na) score of more than 15. We further excluded patients with lactose intolerance, coeliac disease, Irritable bowel syndrome defined by ROME III criteria<sup>49</sup>, antibiotic treatment in the prior 3 months, treatment with nutritional drinks, probiotics or prebiotics within the last 3 months, infectious gastroenteritis within the past 6 weeks, investigator judged that the patient would not have been compliant with the trial medication, pregnancy, known liver disease other than alcohol-related, severe malnutrition, malignancy within the past year before inclusion, except planocellular skin cancer or basocellular skin cancer.

## Randomization and interventions

Patients were 1:1 randomized into ReFerm® or Fresubin® groups using a web-based application, REDCap<sup>50</sup>. The trial was designed as an active-comparator-controlled trial since nutritional support is considered to improve outcomes in patients with advanced liver disease<sup>43,44</sup>. Randomization employed permuted blocks of two and four, stratified by self-reported alcohol abstinence for at least 1 week before inclusion. ReFerm® is a postbiotic product made by fermenting oat gruel composition with *Lactobacillus plantarum* DSM 9843, and it has shown similar effects with both live and heat-killed *Lactobacillus plantarum* DSM 9843<sup>15</sup>. It includes oats, barley malt, lecithin, water, and thiamine, along with microbial metabolites like SCFAs from fermentation. The energy content of 100 mL ReFerm® is 58 kcal (1.6 g protein, 9.8 g carbohydrates, 0.9 g fat), and a daily intake of 2 packages provides 290 kcal. The active comparator, Fresubin® Original, was a standard nutritional support for cirrhosis patients that offers 100 kcal per 100 mL (3.8 g protein, 13.8 g carbohydrates, 3.4 g fat), with a daily intake of 2 packages providing 400 kcal. Patients were instructed to take the assigned product in addition to their regular meals. Both groups adhered to a prespecified routine, increasing their dosage in the first week to allow the digestive system to adapt to the product. From day seven and throughout the remaining trial period, patients had to ingest two bottles a day, which corresponds to 400 mL Fresubin® or 500 mL ReFerm®. Both groups had to drink one dosage before breakfast and one dosage between 4 and 6 PM. If bowel symptoms occurred in relation to the study product, patients were instructed to reduce intake by 50% for at least 2 days, or until the symptoms disappeared. Hereafter, the dosage was gradually increased until the full dosage was achieved. Compliance was monitored during four in-hospital visits through self-reporting compliance and by counting the lids of consumed products. If there was a discrepancy between the reported consumption and the counted lids, patients were asked to explain. In the absence of a satisfactory explanation, the counted lids were used as the measure of compliance. Additionally, nine follow-up

phone calls were made between visits to gather self-reported compliance data. During each compliance assessment, study personnel also evaluated the presence of any side effects. If patients frequently forgot to consume the product, they were offered additional reminders via phone calls or text messages. If patients experienced difficulties with side effects resulting in decreased compliance, the study coordinator considered discontinuing the patient's participation (Fig. S7).

## Trial investigations

At baseline and after 24 weeks of treatment, patients underwent a liver biopsy. Outcome assessment of the baseline and end-of-study biopsy samples ( $\alpha$ -SMA expression) was done by a single expert pathologist who was blinded to treatment group and all clinical data (SD).  $\alpha$ -SMA expression was assessed using automated digital imaging analysis of digitalized immunohistochemically stained liver biopsy sections (a detailed description can be found in Supplementary Material). Liver fibrosis was assessed by a single expert pathologist (GHJ) according to the Kleiner staging system for fibrosis, and grading of lobular inflammation, ballooning, and steatosis was performed according to the NASH Clinical Research Network activity score<sup>51</sup>. Biological material and standard biochemistry were recorded at each of the four in-hospital visits. Alcohol use was quantified by patient reports using predefined questionnaires at each trial visit. Patients were advised to abstain from alcohol per clinical standards.

## Primary outcome

The primary outcome was a between-group comparison of histological reduction of activated HSCs, defined as  $\geq 10\%$  absolute reduction in the percentage positive for  $\alpha$ -SMA expression, from baseline to 24 weeks of treatment. The rationale for choosing this endpoint was that  $\alpha$ -SMA is a marker of activated HSCs. Activated HSCs are the key cellular components in liver collagen accumulation, driving fibrogenesis<sup>30–32</sup>.  $\alpha$ -SMA expression of the baseline and end-of-study biopsy samples was done by a single expert pathologist who was blinded to treatment group and all clinical data (SD). To meet quality criteria for liver biopsies, the sample should be at least ten millimeters long and with at least six portal tracts or the presence of cirrhotic regenerative nodules.  $\alpha$ -SMA was identified immunohistochemically (Ventana Benchmark Ultra autostainer using prediluted Nordic Biosite Clone BS66 and Optiview DAB detection kit)<sup>6</sup>. Stained slides were digitized using a 20 $\times$  objective on a Hamamatsu NanoZoomer 2.0–HT whole slide scanner (Hamamatsu Photonics, Hamamatsu, Japan). Automated digital image quantitation was performed using the Visiopharm Image Analysis Software, version 2018.4 (Hørsholm, Denmark) as previously described<sup>6</sup>. The expression level for  $\alpha$ -SMA was calculated as a percentage of the  $\alpha$ -SMA positive area in relation to the total liver biopsy area<sup>6</sup>.

## Secondary outcomes

All secondary outcomes were between-group comparisons of changes from baseline to after 24 weeks of treatment. Histological outcomes included the absolute change of any alterations in  $\alpha$ -SMA expression, and at least one stage improvement in liver fibrosis with no worsening of hepatic inflammatory activity, and a complete resolution of hepatic inflammatory activity with no worsening of fibrosis. Non-invasive markers of liver fibrosis and steatosis included LSMs using TE, controlled attenuation parameter (CAP), ELF test, N-terminal pro-peptide of type III collagen (PRO-C3), and two-dimensional shear wave elastography (2D-SWE). FibroScan 502 touch®, Echoscens, France, and Aixplorer® (Hologic) were used for TE, CAP, and 2D-SWE assessments, following standard procedures<sup>52,53</sup>. PRO-C3, a fragment of N-terminal type III collagen, was measured by Nordic Bioscience using ELISA. Details on omics analyses are described in the Supplementary.

### Omic analysis

Omic analyses were applied to explore mechanistic pathways, including changes of gut microbiome composition, SCFAs in stool and plasma, plasma proteins, bile acids, amino acids, with other small molecules in stool and plasma, and the plasma lipidome.

### Fecal bacterial metagenomics

Stool samples were collected in connection with the clinical visit at baseline, 4 weeks, 24 weeks (end of intervention), and after a wash-out period of 6–8 weeks. The samples were collected by the participants within 24 h of each visit. Participants were given instructions and materials for sample collection. The sample was collected in sealed test tubes and stored immediately in the participants' freezers. The samples were transported to the hospital as cold as possible using a cooler bag and cooling elements. Upon arrival at the hospital, the sample was stored in a –80 freezer until shipment. The samples were shipped by courier.

### DNA sequencing

DNA extraction from stool samples was carried out employing the Qiagen AllPrep PowerFecal DNA/RNA Kit. The preparation of metagenomic sequencing libraries was conducted using the NEBNext Ultra II DNA Library Prep kit, targeting an insert size of 350–400 bp, and incorporating Dual Index multiplex oligos. The library preparation process utilized a liquid automated system (Beckman Coulter i7 Series). Subsequently, sequencing was performed on an Illumina HiSeq 4000 platform (Illumina, San Diego, CA, USA), generating 2 × 150 bp paired-end reads.

### Metagenomic data processing and quality control

Metagenomic data underwent quality filtering using *ngless* v1.1 to eliminate data of insufficient quality<sup>54</sup>. Nucleotide calls with a Phred score below 25 were excluded from the 3' end. Reads shorter than 45 nucleotides, post low-quality nucleotide removal, were excluded. Identification of reads corresponding to human DNA involved comparing sequence similarity to the human reference genome. Reads with over 90% similarity to the human genome were eliminated to uphold patient privacy rights. Following these processing steps and QC measures, reads were categorized as paired or singles, signifying the presence of both or only the forward and reverse reads in the final dataset, respectively.

Metagenomic reads were analyzed to assess species abundances through the utilization of marker genes (mOTUs v2.5)<sup>55</sup>. Among the detected species, 312 species with average relative abundance >0.1% and detected in >20% of samples, were included in the following analysis. The Shannon diversity of the gut microbiome was estimated using the diversity function in the *vegan* package, and the enterotype<sup>56,57</sup> of each sample was predicted using the "Enterotyper" webserver with the 3-enterotype model based on the partition around medoid option<sup>58</sup>. For functional analysis of the microbiome, metagenomic reads were mapped to the global microbial gene catalog<sup>59</sup> human gut nr95 using BWA-MEM<sup>60</sup> (0.7.17), and the catalog was annotated with *eggnog mapper*<sup>61</sup> (v1.0.3) against the *eggnog* database 5.0<sup>62</sup>, assigning each gene a set of KEGG orthology<sup>63</sup>. The relative abundances of KEGG orthologies were calculated using *gffquant* version v2.9.1 ([https://github.com/cschu/gff\\_quantifier](https://github.com/cschu/gff_quantifier)), where counts of reads aligned to multiple genes were distributed fractionally to the genes. Pathway enrichment analysis was performed using the *GSEA* function in the *clusterProfiler*<sup>64</sup> package in R.

### Plasma cytokines

The Target-96 "Inflammation" and "Cardiovascular II" Panel by Olink Proteomics was employed for the semi-quantitative assessment of 92 cytokines, utilizing proximity extension assay technology based on quantitative polymerase chain reaction (qPCR) extension of

oligonucleotides attached to antibody pairs specific to the target protein. To enhance practicality and minimize batch effects, cohorts were divided into four batches. Within each batch, samples were randomized, and 16 bridging samples were included. Plasma samples with EDTA were thawed on ice, and 40 µL was aliquoted into 96-well plates. Subsequently, the samples were shipped on dry ice to Olink for analysis.

The received raw data (NPX values) from Olink were processed using the *OlinkAnalyze* package in R. Batches were bridged by utilizing the 16 bridging samples in each batch. Samples flagged with QC warnings in the standard Olink QC underwent manual review before a decision was made to either retain or exclude them. Cytokines exhibiting more than 75% missing data across all batches were excluded from further analysis.

### Bile acids, amino acids, and other small molecules

In the plasma analysis, the QQQ method was employed. Sample preparation involved protein precipitation and derivatization. Specifically, 10 µL of a 1 M solution of 5-sulphosalicylic acid dehydrate was added to 30 µL of the plasma sample. After vortex mixing and centrifugation at 10,000 rpm (8 min at 4 °C), 20 µL of the upper phase was collected. Subsequently, 20 µL of the Internal Standard (ISTD) MIX and 6-aminoquinoline-N-hydroxy-succinimidyl carbamate-reagent (AQC reagent) were added, and the samples were vortex mixed and stored at –80 °C until analysis.

The UHPLC system utilized was the 1290 Infinity system from Agilent Technologies, comprising a multi-sampler (maintained at 10 °C), a binary solvent manager, and a column thermostat (maintained at 40 °C). Separations were executed on a Kinetex® F5 column (100 × 2.1 mm, particle size 1.7 µm) from Phenomenex (Torrance, CA, USA), with a flow rate of 0.4 mL min<sup>-1</sup> and an injection volume of 2 µL. Mobile phases included H<sub>2</sub>O + 0.1% HCOOH (A) and ACN:IPA (2:1, v/v) + 0.1% HCOOH (B) for gradient elution. The gradient profile was as follows: from 0 to 1 min 1% B, from 1 to 1.8 min 1–18% B, from 1.8 to 3.4 min 18–21% B, from 3.4 to 7 min 21–65% B, from 7 to 7.1 min 65–100% B, and from 7.1 to 8.9 min 100% B. Each run was succeeded by a 2.5 min re-equilibration period under initial conditions (1% B).

The mass spectrometer employed was a 6460 triple quadrupole system from Agilent Technologies, interfaced with an Agilent Jet Stream electrospray ionization source. Analytes were ionized in positive or negative ion mode based on the properties of each analyte. Data processing was carried out using *MassHunter Quantitative Analysis Software*<sup>65</sup>.

For the analysis of fecal samples, the QQQ method was employed. Initially, 400 µL of methanol was added to 20 mg of fecal samples before homogenization using a *Tissuelyser*. The homogenized samples underwent centrifugation for 10 min at 10,000 rpm, and 250 µL of the resulting supernatant was carefully transferred to a separate Eppendorf tube, where it was subsequently dried under a flow of nitrogen. The dried samples were then reconstituted with 100 µL of a 1:1 water:methanol solution, followed by centrifugation for 3 min at 10,000 rpm. Subsequently, 20 µL of the supernatant was transferred to an LC vial with a 300 µL insert. To this, 20 µL of the Internal Standard (ISTD) MIX and 20 µL of the AQC reagent were added. After vortex mixing, the samples were stored at –80 °C until the time of analysis<sup>66</sup>.

### Short-chain fatty acids

Analysis of SCFAs from both plasma and fecal samples was conducted through a Gas Chromatography-Quadrupole Time-of-Flight (GC-QTOF) system, specifically the Agilent 8890A/7250A, following a previously outlined methodology<sup>54</sup>.

For plasma samples, 140 µL of the internal standard mixture (comprising Acetic acid-d4, Propionic acid-d6, Butyric acid-d8, Undecanoic acid, and 2-Ethylbutyric acid) in MTBE was added to 100 µL of the samples. The samples underwent acidification with Phosphoric acid, followed by vortexing, incubation on ice for 30 min, and

centrifugation for 5 min at 10,000 rpm. The resulting organic phase was subjected to GC-TOF analysis.

In the case of 5 mg fecal samples, 1000  $\mu$ L of the ISTD mix was employed. Similar to the plasma samples, the fecal samples underwent acidification with Phosphoric acid, homogenization using Tissuelyser, incubation on ice for 30 min, and centrifugation for 5 min at 10,000 rpm. Subsequently, the organic phase was filtered using a Millex HV unit and subjected to GC-QTOF analysis.

The chromatographic columns consisted of a methyl-deactivated retention gap (1.5 m  $\times$  0.53 mm i.d.) connected to a 30 m  $\times$  0.25 mm Stabilwax-DA column (phase thickness 0.25  $\mu$ m). A 1  $\mu$ L split injection (1:10) was applied, and Helium served as the carrier gas at a constant flow mode (1 mL/min). The temperature program included an initial phase at 40  $^{\circ}$ C, followed by a ramp of 10  $^{\circ}$ C/min to 200  $^{\circ}$ C, and then a further increase of 25  $^{\circ}$ C/min to 250  $^{\circ}$ C, maintained for 5 min. Data processing was performed using MassHunter Quantitative Analysis software.

### Plasma lipids

Plasma samples (10  $\mu$ L) were combined with 10  $\mu$ L of 0.9% w/v NaCl (aq) and internal standards, which comprised a 120  $\mu$ L chloroform/methanol (2:1) mixture. The lipid-containing chloroform was subjected to analysis using an Agilent ultra-high performance liquid chromatograph coupled with a quadrupole time-of-flight mass spectrometer. The samples were analyzed in a randomized order, with QC pooled plasma samples interspersed at regular intervals throughout the run ( $n=30$  for both positive and negative ionization)<sup>67</sup>. The lipidomics data underwent pre-processing with MZmine2<sup>68</sup>, followed by normalization to internal standard and log transformation. Subsequently, the data were cross-matched with an in-house library.s.

### Animal experimentation

A total of 11 specific pathogen-free male wild-type (WT, C57Bl6/J) mice, aged 12 weeks, were used in this study. The mice were obtained from Charles River Laboratories Research Model and Services, Sulzfeld, Germany. They were housed at 22  $^{\circ}$ C with a 12-h light/dark cycle in individually ventilated cages. ALD was induced by administering intraperitoneal CCl<sub>4</sub> injections twice weekly for 7 weeks. In addition to CCl<sub>4</sub>, the mice received phenobarbital (0.33 g/l) in their drinking water to stimulate cytochrome P-450 metabolic activity. Ethanol was added to their drinking water (4% in week 1, 8% in week 2, and 16% until euthanasia). Water and chow were available *ad libitum*, and further details about the diet are provided in Table S7. The intervention groups received twice daily oral gavage (0.3 mL) of Fresubin<sup>®</sup> or ReFerm<sup>®</sup> for 1 week prior to sacrifice. Age-matched, untreated mice ( $N=3$ ) served as controls for all experiments. The experimental design is visualized in Fig. S8. Before euthanasia, the mice were anesthetized with an intraperitoneal injection of ketamine-xylazine (100 mg ketamine/kg body weight and 10 mg xylazine/kg body weight). Cervical dislocation was used for euthanasia. At organ harvest, liver and serum samples were collected. Liver samples were snap-frozen and stored at  $-80^{\circ}$ C. Blood samples were allowed to clot for 30 min at room temperature and aliquoted after centrifugation at 2000  $\times$  g for 10 min. Serum aliquots were immediately stored at  $-80^{\circ}$ C. All animals received human care in accordance with the criteria outlined in the EU regulations on animal research (2010/63/EU). All experiments were performed in accordance with the German animal protection and welfare law and the guidelines of the animal care facility at the Hospital of the Goethe University Frankfurt and were approved by the responsible local authorities, the Darmstadt regional council (File reference number: FK/2005).

### Quantitative PCR and enzyme-linked immunosorbent assay (ELISA)

Total RNA was extracted using a standard TRIzol-based protocol (TRIzol Reagent, Ambion, Carlsbad, CA, USA). cDNA synthesis and

qPCR were performed as described previously<sup>55</sup>. TaqMan gene expression assays (Thermo Fisher Scientific, Waltham, MA, USA) were used for qPCR according to the manufacturer's protocol on a 7300 Real-Time PCR System (Applied Biosystems, Foster City, CA). Each qPCR analysis included duplicate wells, and appropriate control reactions were performed in all samples. The expression of each gene was calculated by the  $2^{-\Delta\Delta C_t}$  method by Schmittgen and Livak<sup>56</sup>. Gene amplification results were standardized against 18S rRNA expression in each sample, and expression levels were presented as x-fold changes relative to the corresponding control group. A full list of the gene expression assays used is provided in Table S8.

Sandwich enzyme-linked immunosorbent assays for I-FABP (EM1144, FineTest, Wuhan, China) and SIRT2 (A77325, Antibodies.com, Stockholm, Sweden) were performed with murine serum samples. Serum samples were thawed and diluted 1:2 with sample dilution buffer, and all buffers and standards were prepared according to the respective assay protocols. The ELISA protocols were applied in accordance with the manufacturer's specifications. The final step of the protocol is a color change, which is detected at 450 nm on a microplate reader. The concentrations of SIRT2 and I-FABP were calculated referring to the standard curve by applying a four-parameter logistic curve and multiplication of the dilution ratio.

### Statistical analysis

The sample size calculation was based on a 6-month RCT drug trial using candesartan cilexetil in patients with ALD and significant liver fibrosis. Here, an absolute reduction of 5% ( $\pm 7\%$ ) in  $\alpha$ -SMA expression was reported in the intervention group, equivalent to a relative decrease of 17% as described in the protocol<sup>32</sup>. Due to the standard deviation of  $\pm 7\%$ , we decided to consider an absolute reduction in  $\alpha$ -SMA of  $\geq 10\%$  as a clinically relevant response. Anticipating a clinically relevant difference in the proportion of responders ( $\geq 10\%$  absolute reduction in  $\alpha$ -SMA), we anticipated that 15% of participants treated with Fresubin<sup>®</sup> would achieve a clinically relevant  $\alpha$ -SMA response, while 60% of participants treated with ReFerm<sup>®</sup> would achieve the response. Accounting for an expected dropout rate of 20%,  $\alpha$  of 5%, and a power of 80%, 40 patients were needed in the study. However, amid the COVID-19 pandemic, patients were hesitant to visit hospitals due to safety concerns, resulting in a higher dropout rate. Furthermore, the level of advanced liver fibrosis led to two index liver biopsies failing quality criteria. Consequently, on September 15, 2020, the steering committee raised the target number of patients to at least 40 to ensure trial completion.

Baseline data are reported in counts (proportion), median (interquartile range), or mean (SD) for continuous, non-normally distributed, and normally distributed data, respectively. Primary outcome analyses were conducted applying ITT and PP analyses. ITT analysis included all randomized patients, and patients who did not complete the study, resulting in missing outcome data, were categorized as having no effect of treatment, consistent with a prior study<sup>29,57</sup>. The PP population included all randomized patients who completed the trial with paired liver biopsies meeting quality criteria. Secondary outcome analyses were performed using PP-analyses, reporting odds ratios (OR) with 95% confidence intervals (CI) for binary outcomes and mean change from baseline with SD for continuous normally distributed outcomes. In assessing liver stiffness changes, we considered a 20% reduction as clinically significant since such a decrease has been previously linked to a reduced risk of hepatic decompensation<sup>35</sup>. Results were presented as PP analysis without adjustment for covariates unless specified. Adjusting for baseline confounders is generally recommended, but these should be prospectively specified in the statistical analysis plan<sup>58</sup>. In the statistical analysis plan of our study, it was specified that primary analyses would be done unadjusted. However, alcohol abstinence at baseline must be considered the most important

potential confounder, which is why stratification was based on this parameter. At inclusion, there was balance between the groups; no further adjustments were made. To assess treatment effects over time, a general linear model was applied, and Cohen's *d* was used to standardize the estimated treatment effect, adjusted for multiple testing. A two-sided  $P < 0.05$  was considered statistically significant for the clinical data. For omics analysis, the Benjamini-Hochberg procedure was applied with an FDR  $< 0.2$  for multiple testing correction. STATA 18 and R 4.3.1 were used for statistics.

### Reporting summary

Further information on research design is available in the Nature Portfolio Reporting Summary linked to this article.

### Data availability

All results from statistical and bioinformatics analysis are provided in the source data file. Average levels of proteins have been deposited in the Zenodo repository at <https://zenodo.org/records/15083400>. The Shotgun metagenomic data sequenced are publicly available in the European Nucleotide Archive under the accession number PRJEB76668, <https://www.ebi.ac.uk/ena/browser/view/PRJEB76668>. In line with the current regulation of the General Data Protection Regulation (<https://gdpr-info.eu/>) to maintain patient confidentiality, individual-level clinical and further omics data generated in this study cannot be made publicly available. Clinical and molecular datasets are available from the authors upon request by contacting J.K.H. at [Johanne.kragh.hansen@rsyd.dk](mailto:Johanne.kragh.hansen@rsyd.dk). Access to the data can be granted through the Danish Data Protection Agency and the ethics committee for the Region of Southern Denmark by obtaining proper approvals and in accordance with patient information and processing agreements. The time frame for response to requests from the authors is within 1 month. When applying and processing data, restrictions apply: (1) a data-processing agreement must be signed between the data controller and processor; (2) data must not be processed for purposes other than statistical and scientific studies; (3) personal data must be deleted, anonymized and destroyed at the end of investigation; and (4) data must not be passed on to a third party or individuals who are not authorized to access the data. Source data are provided with this paper.

### References

- Karlsen, T. H. et al. The EASL-Lancet Liver Commission: protecting the next generation of Europeans against liver disease complications and premature mortality. *Lancet* **399**, 61–116 (2022).
- Lynch, S. V. & Pedersen, O. The human intestinal microbiome in health and disease. *N. Engl. J. Med.* **375**, 2369–2379 (2016).
- Bajaj, J. S. et al. Altered profile of human gut microbiome is associated with cirrhosis and its complications. *J. Hepatol.* **60**, 940–947 (2014).
- Puche, J. E., Saiman, Y. & Friedman, S. L. Hepatic stellate cells and liver fibrosis. *Compr. Physiol.* **3**, 1473–1492 (2013).
- Hautekeer, M. L. & Geerts, A. The hepatic stellate (Ito) cell: its role in human liver disease. *Virchows Arch.* **430**, 195–207 (1997).
- Sørensen, M. D. et al. Stage-dependent expression of fibrogenic markers in alcohol-related liver disease. *Pathol. Res. Pract.* **231**, 153798 (2022).
- Enzan, H. et al. Immunohistochemical identification of Ito cells and their myofibroblastic transformation in adult human liver. *Virchows Arch.* **424**, 249–256 (1994).
- Tranah, T. H., Edwards, L. A., Schnabl, B. & Shawcross, D. L. Targeting the gut-liver-immune axis to treat cirrhosis. *Gut* **70**, 982–994 (2021).
- Trebicka, J., Bork, P., Krag, A. & Arumugam, M. Utilizing the gut microbiome in decompensated cirrhosis and acute-on-chronic liver failure. *Nat. Rev. Gastroenterol. Hepatol.* **18**, 167–180 (2021).
- Jung, J. H., Kim, S. E., Suk, K. T. & Kim, D. J. Gut microbiota-modulating agents in alcoholic liver disease: Links between host metabolism and gut microbiota. *Front. Med.* **9**, 913842 (2022).
- Albillos, A., de Gottardi, A. & Rescigno, M. The gut-liver axis in liver disease: Pathophysiological basis for therapy. *J. Hepatol.* **72**, 558–577 (2020).
- Adachi, Y., Moore, L. E., Bradford, B. U., Gao, W. & Thurman, R. G. Antibiotics prevent liver injury in rats following long-term exposure to ethanol. *Gastroenterology* **108**, 218–224 (1995).
- Salminen, S. et al. The International Scientific Association of Probiotics and Prebiotics (ISAPP) consensus statement on the definition and scope of postbiotics. *Nat. Rev. Gastroenterol. Hepatol.* **18**, 649–667 (2021).
- Hsu, C. L. & Schnabl, B. The gut-liver axis and gut microbiota in health and liver disease. *Nat. Rev. Microbiol.* **21**, 719–733 (2023).
- Bednarska, O. et al. A postbiotic fermented oat gruel may have a beneficial effect on the colonic mucosal barrier in patients with irritable bowel syndrome. *Front. Nutr.* **9**, 1004084 (2022).
- Krag, A. et al. Profermin is efficacious in patients with active ulcerative colitis—a randomized controlled trial. *Inflamm. Bowel Dis.* **19**, 2584–2592 (2013).
- Jaeger, J. W. et al. Microbiota modulation by dietary oat beta-glucan prevents steatotic liver disease progression. *JHEP Rep.* **6**, 100987 (2024).
- Louvet, A. et al. Low alcohol consumption influences outcomes in individuals with alcohol-related compensated cirrhosis in a French multicenter cohort. *J. Hepatol.* **78**, 501–512 (2023).
- Thorhaug, K. H. et al. Using liver stiffness to predict and monitor the risk of decompensation and mortality in patients with alcohol-related liver disease. *J. Hepatol.* **81**, 23–32 (2024).
- Kim, D. et al. Decline in annual mortality of hepatitis C virus-related hepatocellular carcinoma in the United States, from 2009 to 2018. *Gastroenterology* **159**, 1558–1560 e2 (2020).
- Israelsen, M. et al. Impact of acute alcohol consumption on circulating microbiome in asymptomatic alcohol-related liver disease. *Gut* (2023).
- Qin, N. et al. Alterations of the human gut microbiome in liver cirrhosis. *Nature* **513**, 59–64 (2014).
- Leclercq, S. et al. Intestinal permeability, gut-bacterial dysbiosis, and behavioral markers of alcohol-dependence severity. *Proc. Natl. Acad. Sci. USA* **111**, E4485–E4493 (2014).
- Parlesak, A., Schäfer, C., Schütz, T., Bode, J. C. & Bode, C. Increased intestinal permeability to macromolecules and endotoxemia in patients with chronic alcohol abuse in different stages of alcohol-induced liver disease. *J. Hepatol.* **32**, 742–747 (2000).
- Schoultz, I. & Keita, Å. V. The intestinal barrier and current techniques for the assessment of gut permeability. *Cells* **9**, 1909 (2020).
- Lau, E. et al. The role of I-FABP as a biomarker of intestinal barrier dysfunction driven by gut microbiota changes in obesity. *Nutr. Metab.* **13**, 31 (2016).
- Graupera, I. et al. Adipocyte fatty-acid binding protein is over-expressed in cirrhosis and correlates with clinical outcomes. *Sci. Rep.* **7**, 1829 (2017).
- Patel, V. C. et al. Rifaximin-alpha reduces gut-derived inflammation and mucin degradation in cirrhosis and encephalopathy: RIFSYS randomised controlled trial. *J. Hepatol.* **76**, 332–342 (2022).
- Israelsen, M. et al. Rifaximin- $\alpha$  for liver fibrosis in patients with alcohol-related liver disease (GALA-RIF): a randomised, double-blind, placebo-controlled, phase 2 trial. *Lancet Gastroenterol. Hepatol.* **8**, 523–532 (2023).
- Kisseleva, T. et al. Myofibroblasts revert to an inactive phenotype during regression of liver fibrosis. *Proc. Natl. Acad. Sci. USA* **109**, 9448–9453 (2012).
- Carpino, G. et al. Alpha-SMA expression in hepatic stellate cells and quantitative analysis of hepatic fibrosis in cirrhosis and in recurrent

- chronic hepatitis after liver transplantation. *Dig. Liver Dis.* **37**, 349–356 (2005).
32. Kim, M. Y. et al. Beneficial effects of candesartan, an angiotensin-blocking agent, on compensated alcoholic liver fibrosis—a randomized open-label controlled study. *Liver Int.* **32**, 977–987 (2012).
  33. Sanyal, A. J. et al. Cirrhosis regression is associated with improved clinical outcomes in patients with nonalcoholic steatohepatitis. *Hepatology* **75**, 1235–1246 (2022).
  34. Johansen, S. et al. Validation of scores of PRO-C3 to predict liver-related events in alcohol-related liver disease. *Liver Int.* **43**, 1486–1496 (2023).
  35. Semmler, G. et al. Dynamics in liver stiffness measurements predict outcomes in advanced chronic liver disease. *Gastroenterology* **165**, 1041–1052 (2023).
  36. Trinh, V. Q. et al. Hepatic stellate cells maintain liver homeostasis through paracrine neurotrophin-3 signaling that induces hepatocyte proliferation. *Sci. Signal.* **16**, eadf6696 (2023).
  37. Yang, Z. et al. Neurotrophin3 promotes hepatocellular carcinoma apoptosis through the JNK and P38 MAPK pathways. *Int. J. Biol. Sci.* **18**, 5963–5977 (2022).
  38. Zhang, Y. et al. SIRT2-mediated deacetylation and deubiquitination of C/EBP $\beta$  prevents ethanol-induced liver injury. *Cell Discov.* **7**, 93 (2021).
  39. Edwards, L. A. et al. Delineation of the innate and adaptive T-cell immune outcome in the human host in response to *Campylobacter jejuni* infection. *PLoS ONE* **5**, e15398 (2010).
  40. Patel, V. C. et al. Rifaximin- $\alpha$  reduces gut-derived inflammation and mucin degradation in cirrhosis and encephalopathy: RIFSYS randomised controlled trial. *J. Hepatol.* **76**, 332–342 (2022).
  41. Fischer, J. et al. Leptin signaling impairs macrophage defenses against *Salmonella Typhimurium*. *Proc. Natl. Acad. Sci. USA* **116**, 16551–16560 (2019).
  42. Macnaughtan, J. et al. A double-blind, randomized placebo-controlled trial of probiotic *Lactobacillus casei* Shirota in stable cirrhotic patients. *Nutrients* **12**, 1651 (2020).
  43. Fialla, A. D., Israelsen, M., Hamberg, O., Krag, A. & Gluud, L. L. Nutritional therapy in cirrhosis or alcoholic hepatitis: a systematic review and meta-analysis. *Liver Int.* **35**, 2072–2078 (2015).
  44. Bischoff, S. C. et al. ESPEN practical guideline: clinical nutrition in liver disease. *Clin. Nutr.* **39**, 3533–3562 (2020).
  45. Lee, M. J. A review of liver fibrosis and cirrhosis regression. *J. Pathol. Transl. Med.* **57**, 189–195 (2023).
  46. Rinella, M. E. et al. A multisociety Delphi consensus statement on new fatty liver disease nomenclature. *Hepatology* **78**, 1966–1986 (2023).
  47. Israelsen, M. et al. Validation of the new nomenclature of steatotic liver disease in patients with a history of excessive alcohol intake: an analysis of data from a prospective cohort study. *Lancet Gastroenterol. Hepatol.* **9**, 218–228 (2024).
  48. Krag, A., Israelsen, H., von Ryberg, B., Andersen, K. K. & Bendtsen, F. Safety and efficacy of Profermin<sup>®</sup> to induce remission in ulcerative colitis. *World J. Gastroenterol.* **18**, 1773–1780 (2012).
  49. Drossman, D. A. Rome III: the new criteria. *Chin. J. Dig. Dis.* **7**, 181–185 (2006).
  50. Harris, P. A. et al. The REDCap consortium: building an international community of software platform partners. *J. Biomed. Inf.* **95**, 103208 (2019).
  51. Kleiner, D. E. et al. Design and validation of a histological scoring system for nonalcoholic fatty liver disease. *Hepatology* **41**, 1313–1321 (2005).
  52. Dietrich, C. F. et al. EFSUMB guidelines and recommendations on the clinical use of liver ultrasound elastography, update 2017 (long version). *Ultraschall Med.* **38**, e48 (2017).
  53. EASL Clinical Practice Guidelines on non-invasive tests for evaluation of liver disease severity and prognosis—2021 update. *J. Hepatol.* **75**, 659–689 (2021).
  54. Lotti, C. et al. Development of a fast and cost-effective gas chromatography-mass spectrometry method for the quantification of short-chain and medium-chain fatty acids in human biofluids. *Anal. Bioanal. Chem.* **409**, 5555–5567 (2017).
  55. Brol, M. J. et al. Combination of CCl<sub>4</sub>(4) with alcoholic and metabolic injuries mimics human liver fibrosis. *Am. J. Physiol. Gastrointest. Liver Physiol.* **317**, G182–g94 (2019).
  56. Schmittgen, T. D. & Livak, K. J. Analyzing real-time PCR data by the comparative C(T) method. *Nat. Protoc.* **3**, 1101–1108 (2008).
  57. Newsome, P. N. et al. A placebo-controlled trial of subcutaneous semaglutide in nonalcoholic steatohepatitis. *N. Engl. J. Med.* **384**, 1113–1124 (2021).
  58. Holmberg, M. J. & Andersen, L. W. Adjustment for baseline characteristics in randomized clinical trials. *JAMA* **328**, 2155–2156 (2022).
  59. Coelho, L. P. et al. Towards the biogeography of prokaryotic genes. *Nature* **601**, 252–256 (2022).
  60. Li, H. & Durbin, R. Fast and accurate short read alignment with Burrows-Wheeler transform. *Bioinformatics* **25**, 1754–60 (2009).
  61. Cantalapiedra, C. P., Hernández-Plaza, A., Letunic, I., Bork, P. & Huerta-Cepas, J. eggNOG-mapper v2: Functional Annotation, Orthology Assignments, and Domain Prediction at the Metagenomic Scale. *Mol. Biol. Evol.* **38**, 5825–5829 (2021).
  62. Huerta-Cepas, J. et al. eggNOG 5.0: a hierarchical, functionally and phylogenetically annotated orthology resource based on 5090 organisms and 2502 viruses. *Nucleic Acids Res.* **47**, D309–D314 (2019).
  63. Kanehisa, M., Furumichi, M., Sato, Y., Kawashima, M. & Ishiguro-Watanabe, M. KEGG for taxonomy-based analysis of pathways and genomes. *Nucleic Acids Res.* **51**, D587–D592 (2023).
  64. Wu, T. et al. clusterProfiler 4.0: A universal enrichment tool for interpreting omics data. *Innovation* **2**, 100141 (2021).
  65. Ahonen, L. et al. Targeted Clinical Metabolite Profiling Platform for the Stratification of Diabetic Patients. *Metabolites* **9**, 184 (2019).
  66. Zawadzki, A. et al. High-Throughput UHPLC-MS to Screen Metabolites in Feces for Gut Metabolic Health. *Metabolites* **12**, 211 (2022).
  67. Israelsen, M. et al. Comprehensive lipidomics reveals phenotypic differences in hepatic lipid turnover in ALD and NAFLD during alcohol intoxication. *JHEP Rep.* **3**, 100325 (2021).
  68. Pluskal, T., Castillo, S., Villar-Briones, A. & Oresic, M. MZmine 2: modular framework for processing, visualizing, and analyzing mass spectrometry-based molecular profile data. *BMC Bioinforma.* **11**, 395 (2010).

## Acknowledgements

The authors thank all participants in this study. Furthermore, the authors thank Louise Just, Lise Ryborg, and Helene Bæk Juel for Consortia project coordination; Vibeke Nielsen, Simon Langkjær Sørensen, Maria Fogt, Helle Lindholm Schnefeld, Julie Hansen and the entire staff at Odense Liver Research Centre; hepatology nurse specialists Trine Møller, Charlotte Damby Jensen, Minna Ingham, Line Jensen, Line Murrekilde, Kirsten Dalhøj, and all the staff at Department of Gastroenterology and Hepatology; Anette Tyrsted and Lea Grip from the Department of Clinical Biochemistry and Pharmacology at Odense University Hospital; the EMBL Genomics Core Facility; and the Department of Open Patient Data Explorative Network, Marianne Bergman from the Biochemical Department, Lillebaelt Hospital. The authors also thank lab technician Lone Christiansen at the Department of Pathology at Odense University Hospital for the immunohistochemical stainings ( $\alpha$ -SMA). We are further very grateful to Elke Weber, Sonja Heinsius, and Marlen Kleppe for excellent technical assistance. Funded by the EU Horizon 2020 program (GALAXY, grant 668031) and Novo Nordisk Foundation (MicroLiver, NNF15OC0016692). This project received funding from the European Union's Horizon 2020 research and innovation program for the GALAXY project under grant agreement number 668031. The study was

supported by the Challenge Grant MicrobLiver grant number NNF15OC0016692 from the Novo Nordisk Foundation.

## Author contributions

M.I., H.I., M.T., and A.K. conceived the study. J.K.H., S.N., S.E.S., P.A., C.D.H., M.J.B., S.K., R.S., F.E.U., K.S., I.F.V., K.P.L., K.H.T., M.I.K., G.H.J., S.D., D.J.L., E.S., T.S., A.Z., M.Ka., and M.Ku. curated the data. J.K.H., S.N., S.E.S., P.A., and C.D.H. did the formal analysis. T.H. and A.K. acquired the funding. J.K.H., C.D.H., K.P.L., K.H.T., N.T., and J.M.J. did the investigation. M.I., M.T., and A.K. devised the methodology. J.K.H. and M.T. did the project administration. L.J.J., J.T., C.L.Q., P.B., M.A., M.T., T.H., and A.K. supervised the study. J.K.H., S.N., S.E.S., P.A., and S.J. did the data visualization. J.K.H., M.I., C.D.H., M.T., and A.K. wrote the original draft. All authors reviewed and edited the manuscript. All authors approved the final manuscript before submission. All authors had access to the data in the study and had responsibility for the final decision to submit for publication.

## Competing interests

J.K.H. has received a speaker's fee from Norgine A/S. M.I.'s father and co-author, H.I., is full-time employed and a stockholder at Nordic Rebalance that produces ReFerm®. M.I. is not employed and is not a stockholder in the company. S.E.S. was funded by the NNF Copenhagen Bioscience PhD Program (grant no. NNF18CC0033668). C.D.H.: Received speaker's fee from Novo Nordisk. K.S. is funded by the Novo Nordisk Foundation Excellence Emerging Investigator Grant—Endocrinology and Metabolism 2022 (grant no. NNF 0074491). Involved in various projects with funding from or directly with Novo Nordisk A/S, all outside the submitted work. K.P.L. has received a speaker's fee from Siemens and Novo Nordisk and is a board member and co-founder of Evido. D.J.L. and M.Ka. are full-time employees and stockholders at Nordic Bioscience. A.Z. is a full-time employee of Nordic Bioscience. L.J.J. is funded by grants from the Novo Nordisk Foundation (grant numbers NNF14CC0001 and NNF21OC0068988) and has a paid position on the scientific advisory board of ZS Associates unrelated to the submitted work. J.T. has received speaking and/or consulting fees from Versantis, Gore, Boehringer Ingelheim, Alexion, Falk, Grifols, CSL Behring, and Genfit. M.Ka. is a full-time employee and stockholder at Nordic Bioscience. H.I. is a full-time employee and stockholder at Nordic Rebalance that produces ReFerm®. T.H. Stockholder at Novo Nordisk. Research support; Novo Nordisk, GSK. M.T. is funded by a grant from the Novo Nordisk Foundation (DECIDE, grant number NNF20OC0059393). Received speaker's fee from Novo Nordisk, Echosens, Madrigal, and Takeda. Advisory fee from Boehringer Ingelheim, Astra Zeneca, Novo Nordisk, and GSK. Co-founder of Evido.

Received an investigator-initiated grant from GSK. A.K. has served as a speaker for Novo Nordisk, Norgine, Siemens, and Nordic Bioscience and participated in advisory boards for Norgine, Siemens, Resalis Therapeutics, Boehringer Ingelheim, and Novo Nordisk, all outside the submitted work. Research support: Norgine, Siemens, Nordic Bioscience, Astra, Echosens. Board member and co-founder of Evido. All other authors declare no competing interests.

## Additional information

**Supplementary information** The online version contains supplementary material available at <https://doi.org/10.1038/s41467-025-60755-9>.

**Correspondence** and requests for materials should be addressed to Aleksander Krag.

**Peer review information** *Nature Communications* thanks Emidio Scarpellini and the other anonymous reviewer(s) for their contribution to the peer review of this work. A peer review file is available.

**Reprints and permissions information** is available at <http://www.nature.com/reprints>

**Publisher's note** Springer Nature remains neutral with regard to jurisdictional claims in published maps and institutional affiliations.

**Open Access** This article is licensed under a Creative Commons Attribution-NonCommercial-NoDerivatives 4.0 International License, which permits any non-commercial use, sharing, distribution and reproduction in any medium or format, as long as you give appropriate credit to the original author(s) and the source, provide a link to the Creative Commons licence, and indicate if you modified the licensed material. You do not have permission under this licence to share adapted material derived from this article or parts of it. The images or other third party material in this article are included in the article's Creative Commons licence, unless indicated otherwise in a credit line to the material. If material is not included in the article's Creative Commons licence and your intended use is not permitted by statutory regulation or exceeds the permitted use, you will need to obtain permission directly from the copyright holder. To view a copy of this licence, visit <http://creativecommons.org/licenses/by-nc-nd/4.0/>.

© The Author(s) 2025

Johanne K. Hansen<sup>1,2</sup>, Mads Israelsen<sup>1,2</sup>, Suguru Nishijima<sup>3</sup>, Sara E. Stinson<sup>4</sup>, Peter Andersen<sup>1</sup>, Stine Johansen<sup>1,2</sup>, Camilla D. Hansen<sup>1,2</sup>, Maximilian Joseph Brol<sup>5</sup>, Sabine Klein<sup>5</sup>, Robert Schierwagen<sup>5</sup>, Frank Erhard Uschner<sup>5</sup>, Karolina Sulek<sup>6</sup>, Ida F. Villesen<sup>1,2</sup>, Katrine P. Lindvig<sup>1,2</sup>, Katrine H. Thorhauge<sup>1,2</sup>, Nikolaj Torp<sup>1,2</sup>, Jane M. Jensen<sup>1</sup>, Marisa Isabell Keller<sup>3</sup>, Gitte H. Jensen<sup>7</sup>, Sönke Detlefsen<sup>2,7</sup>, Diana J. Leeming<sup>8</sup>, Evelina Stankevic<sup>4</sup>, Tommi Suviavaara<sup>6</sup>, Andressa Zawadzki<sup>6,8</sup>, Michael Kuhn<sup>3</sup>, Lars Juhl Jensen<sup>9</sup>, Morten Karsdal<sup>8</sup>, Jonel Trebicka<sup>1,5,10</sup>, Hans Israelsen<sup>11</sup>, Cristina Legido-Quigley<sup>6,12</sup>, Peer Bork<sup>3,13,14</sup>, Manimozhiyan Arumugam<sup>1,4</sup>, Torben Hansen<sup>4</sup>, Maja Thiele<sup>1,2,15</sup> & Aleksander Krag<sup>1,2,15</sup> ✉

<sup>1</sup>Department of Gastroenterology and Hepatology, Centre for Liver Research, Odense University Hospital, Odense, Denmark. <sup>2</sup>Department of Clinical Research, Faculty of Health Sciences, University of Southern Denmark, Odense, Denmark. <sup>3</sup>Molecular Systems Biology Unit, European Molecular Biology Laboratory, Heidelberg, Germany. <sup>4</sup>Novo Nordisk Foundation Center for Basic Metabolic Research, Faculty of Health and Medical Sciences, University of Copenhagen, Copenhagen, Denmark. <sup>5</sup>Department of Internal Medicine B, University of Münster, Münster, Germany. <sup>6</sup>Steno Diabetes Center Copenhagen, Herlev, Denmark. <sup>7</sup>Department of Pathology, Odense University Hospital, Odense, Denmark. <sup>8</sup>Nordic Bioscience A/S, Biomarkers & Research,

Herlev, Denmark. <sup>9</sup>Novo Nordisk Foundation Center for Protein Research, CPR, University of Copenhagen, Copenhagen, Denmark. <sup>10</sup>European Foundation for the Study of Chronic Liver Failure, Barcelona, Spain. <sup>11</sup>Nordic Rebalance A/S, Hillerød, Denmark. <sup>12</sup>Institute of Pharmaceutical Science, King's College London, London, UK. <sup>13</sup>Max Delbrück Centre for Molecular Medicine, Berlin, Germany. <sup>14</sup>Department of Bioinformatics, Biocenter, University of Würzburg, Würzburg, Germany. <sup>15</sup>These authors jointly supervised this work: Maja Thiele, Aleksander Krag. ✉ e-mail: [Aleksander.Krag@rsyd.dk](mailto:Aleksander.Krag@rsyd.dk)